J Mater Sci: Mater Med (2007) 18:1735–1743
DOI 10.1007/s10856-007-3069-7

A novel route for synthesis of nanocrystalline hydroxyapatite from eggshell waste

D. Siva Rama Krishna · A. Siddharthan · S. K. Seshadri · T. S. Sampath Kumar

Received: 6 December 2005 / Accepted: 31 May 2006 / Published online: 5 May 2007

Abstract The eggshell waste has been value engineered to a nanocrystalline hydroxyapatite (HA) by microwave processing. To highlight the advantages of eggshell as calcium precursor in the synthesis of HA (OHA), synthetic calcium hydroxide was also used to form HA (SHA) following similar procedure and were compared with a commercially available pure HA (CHA). All the HAs were characterized by X-ray powder diffraction (XRD) method, Fourier transform infrared (FT-IR) spectroscopy, scanning electron microscopy (SEM), transmission electron microscopy (TEM) and specific surface area measurements. Nanocrystalline nature of OHA is revealed through characteristic broad peaks in XRD patterns, platelets of length 33–50 nm and width 8–14 nm in TEM micrograph and size calculations from specific surface area measurements. FT-IR spectra showed characteristic bands of HA and additionally peaks of carbonate ions. The cell parameter calculations suggest the formation of carbonated HA of B-type. The OHA exhibits superior sinterability in terms of hardness and density than both SHA and CHA may be due to larger surface area of its spherulite structure. The in vitro dissolution study shows longer stability in phosphate buffer and cell culture test using osteoblast cells establishes biocompatibility of OHA.

D. Siva Rama Krishna · A. Siddharthan · S. K. Seshadri · T. S. Sampath Kumar (✉)
Department of Metallurgical & Materials Engineering, Indian Institute of Technology Madras, Chennai 600 036, India
e-mail: tssk@iitm.ac.in

Present Address:
D. Siva Rama Krishna
School of Materials Engineering, Nanyang Technological University, Singapore 639798, Singapore

Introduction

Natural biomaterials like bone substitutes from bovine source, cardiovascular prostheses of biological origin, wound dressings made of biologically derived calcium alginate, collagen, chitin etc., have recently started to surpass the synthetic biomaterials by providing an abundant source for novel biomedical applications [1]. Hydroxyapatite (HA), the inorganic constituent of bone and hard tissues, is one of the most widely used biomaterials for reconstruction of the skeleton. Commercially available HAs are expensive due to the use of high purity reagents [2, 3]. The HA derived from natural materials such as bovine bone [3–5], fish bone [6] or coral [7, 8] has the advantage that they inherit some properties of the raw materials such as the pore structure, carbonated HA etc. However, problems do arise due to the variability of physical and chemical properties of the raw material [3]. The eggshell represents 11% of the total weight of the egg and is composed predominantly of calcium carbonate (94%), calcium phosphate (1%), organic matter (4%) and magnesium carbonate (1%). Though these are occasionally used as a fertilizer due to their high content of calcium and nitrogen [9], most of these are discarded as waste. By utilizing this organic waste, namely eggshell, the cost of high quality calcium source for preparation of HA can be avoided and at the same time recycling of eggshell also can be taken care of [9]. Eggshell after treating with dilute sodium hypochlorite has been studied for application in facial reconstructive surgery [2]. However calcium

carbonate is unsuitable for most implant purposes due to its high dissolution rate and poor stability [1]. HA materials which were prepared from bovine and human resources by treating them with dilute HCI acid is not safe as some diseases can survive all controlled processes. For example prions, a small proteinaceous infectious particle, can survive such processes. High temperature calcinations above 850 °C could solve this problem of transmission of diseases [10]. HA has been produced from eggshell at elevated temperature of 1,050 °C, but contained minute fractions of other calcium compounds [9]. Highly sinterable β-tricalcium phosphate (β-TCP) has been synthesized from eggshell by a wet chemical method followed by heating at high temperature and the ball-milled β-TCP was fully densified at 1,200 °C [11].

Natural bone minerals are nanostructed non-stoichiometric HA of dimensions 20 nm in diameter and 50 nm long with substitution of ions like magnesium, fluoride and carbonate. From bionics viewpoint, synthetic apatites to be used for repairing damaged hard tissues are expected to have characteristics closer to those of biological apatite in both composition and structure [12]. Nanocrystalline HA has been shown to exhibit enhanced bioactivity [13]. Microwave synthesis is an efficient and simple method for preparing nanocrystalline inorganic materials with narrow distribution of particle size and shape in a rapid manner [14]. In recent years, there have been many reports of microwave synthesis of HA and influence of process parameters on its thermal stability, shape and size [15–21]. Production of calcium carbonate and biphasic calcium phosphate materials by microwave processing of natural aragonite and calcite has also been reported [22].

In this study (based on which a patent has been applied in India), a novel yet simple method to convert hen's eggshell into nanocrystalline HA by microwave processing has been presented for the first time to the best of the knowledge of the authors. The physico-chemical characterizations of the nano HA powder were carried out. Since HA can also been used in its ceramic form, fabricated by sintering [23], sinterability studies of the synthesized nano HA have been carried out. Dissolution rate and in vitro cell culture studies were undertaken. To highlight the advantages of using eggshell as a calcium source for the synthesis of HA (OHA), the results were compared with HA (SHA) prepared using synthetic calcium hydroxide by similar microwave processing as well as with a commercially available high purity HA (CHA).

Materials and methods

Hen's eggshells were washed thoroughly and heated in a box furnace at 900 °C for 2 h to decompose organic matter and convert the calcium carbonate to calcium oxide which in turn on exposure to atmosphere forms calcium hydroxide. The product was finely ground in an agate pestle and mortar. The calcium hydroxide was weighed and mixed with distilled water to form 0.3 M suspension and reacted with 0.5 M diammonium hydrogen phosphate solution corresponding to the stoichiometric ratio of Ca/P = 1.67. The mixed reactants were irradiated in a domestic microwave oven (BPL India, 2.45 GHz, 800 W power). The microwave power and duration of exposure were optimized to prevent spilling out of the container. The product was then washed repeatedly with distilled water to remove unwanted ions and dried overnight in an oven at 100 °C. This method of OHA synthesis from eggshell has been repeated several times and found to be reproducible. The SHA was prepared in an identical manner by microwave processing using synthetic calcium hydroxide (Analytical grade, Merck, Germany) while the high purity CHA was procured commercially (Aldrich, USA). A small amount of all the samples were heated at 900 °C for 2 h and furnace cooled to improve the crystallinity and to check the purity.

The X-ray powder diffraction (XRD) analysis of the samples was done (Shimadzu, XD-D1, Japan) in reflection mode with Cu Kα radiation. The functional groups present in HA were ascertained by Fourier transform infrared spectroscopy (FT-IR). The FT-IR spectra were obtained over the region 400–4,000 cm^{-1} using KBr pellet technique with spectral resolution of 4 cm^{-1}. The crystalline size and morphology were analysed in a transmission electron microscope (TEM) operated at 120 KeV (Philips CM12wSTEM, Netherlands). TEM specimens were prepared by depositing a few drops of HA dispersed in ethanol on carbon coated copper grid. The specific surface area of the HA powder were measured using surface area analyzer (CE instruments, Sorpomatic, India) based on Brunauer Emmett and Teller (BET) gas adsorption method. The simultaneous thermo gravimetric analysis (TG) and differential thermal analysis (DTA) of the organic waste was performed (Netzsch STA 409 thermal analyzer, Germany) in nitrogen atmosphere from room temperature to 1,400 °C at a heating rate of 10 °C/min.

Sintering studies were carried out on samples of HA pellets (10 mm diameter and 3 mm height) compacted at a pressure of 80 MPa, at various temperatures from 800 to 1,250 °C for 12 h in air. The sintered pellets were subjected to XRD, hardness and density measurements. Density was determined using Archimedes principle with water as liquid medium using the formula: $\rho_2 = A/P \cdot \rho_0$ (g/m^3), where ρ_2 is the density of the pellet, ρ_0 is the density of the liquid, A is weight of the pellet and P is the difference in weights of the pellet before and after immersion in the liquid. The hardness values were measured using a micro hardness tester (Shimadzu N 0 4800, Japan) at a load of 300 g applied for 10 s on the finely

polished surface of the sintered pellets. The microhardness was calculated from the indentations using the formula: Hv = 1.854 L/d^2, where Hv is the Vickers hardness number, L is the applied load in kg and d is the diagonal length of the square indentation in mm. The morphology of HA powder and fractured surface of sintered HA were studied using scanning electron microscope (JEOL JSM 5410 & JSM 5300, Japan) after coating with a gold film.

The dissolution study of HA powder was carried out in phosphate buffer solution (at a ratio of 1 mg/ml) of pH 7.2 maintained at 37 °C by measuring the pH at regular intervals for 1 week. The in vitro cytotoxicity test was done as per direct contact method (ISO 10993–5, 1999) using osteoblast cells maintained in minimum essential media supplemented with foetal bovine serum. These cells were seeded onto 900 °C sintered HA pellets of 4 mm diameter and 2 mm thickness for 24 h and viewed under optical microscope. High-density polyethylene and copper were used as negative and positive control samples respectively.

Results and discussion

Eggshell has a three layer structure consisting of outermost protein rich cuticle layer, the spongeous middle layer and the inner lamellar layer. Both the middle and inner layers form a matrix constituted by protein fibres bonded to calcium carbonate (calcite) crystals in the proportion of 1:50 [9]. So, to evaluate the decomposition behaviour of the organic matter and calcium carbonate, the thermal analysis of eggshell was carried out. The simultaneous TG-DTA thermogram of eggshell (Fig. 1) shows a weight loss of 45% between 50 and 830 °C and a sharp endothermic peak at 830 °C in DTA, which may be due to the decomposition of calcium carbonate to calcium oxide. This calcium oxide on exposure to atmosphere would convert to calcium hydroxide. The XRD pattern of powdered eggshell (Fig. 2a) shows peaks corresponding to calcium carbonate (JCPDS 5-0586) only while the heat-treated eggshell (Fig. 2b) shows peaks corresponding to calcium hydroxide (JCPDS 4-0733). Trace amounts of carbonate peaks observed might be due to reaction with atmosphere to form calcium carbonate while being furnace cooled as was observed in the heat treatment of corals [8].

The XRD pattern of oven dried OHA was found to be similar to that of oven dried SHA and as received CHA, exhibiting peaks corresponding to HA (JCPDS 9-432) only while the results of heat-treated samples of OHA and SHA show increased crystallinity with sharper peaks. Appearance of new peaks corresponding to β-TCP (JCPDS 9-169) was observed in case of CHA as shown in Fig. 3. This may be due to its non-stoichiometric composition resulting in decomposition at 900 °C [24]. The lattice parameters calculated from XRD data by least squares fit method as listed in Table 1, indicates that the values are comparable with reported values of a-axis 9.418 Å and c-axis 6.884 Å (JCPDS 9-432). The broad peaks observed in Fig. 3 indicate nanocrystalline nature of the synthesized powder. The average crystallite size of the powder was estimated using the Scherrer formula $t = K\,\lambda/B\,\mathrm{Cos}\theta$, where t is the average crystallite size (nm); K is the shape factor ($K = 0.9$); λ is the wavelength of the X-rays ($\lambda = 1.54056$ Å for Cu Kα radiation); B is the full width at half maximum (radian) and θ is the Bragg's diffraction angle (°). The diffraction peak at 25.9° (2θ) was chosen for calculation of the crystallite size, as it is isolated from others. This peak corresponds to (002) Miller plane family. The (002) peaks of oven dried OHA and SHA are broader than CHA indicating

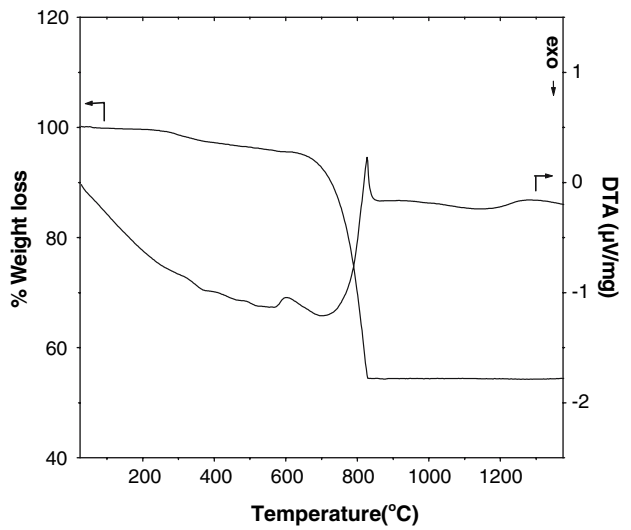

Fig. 1 TG-DTA thermogram of eggshell

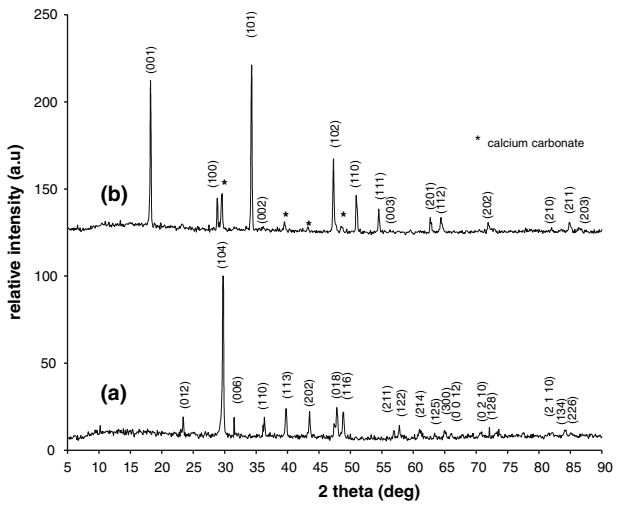

Fig. 2 XRD pattern of powdered eggshell (**a**) and after heating at 900 °C (**b**)

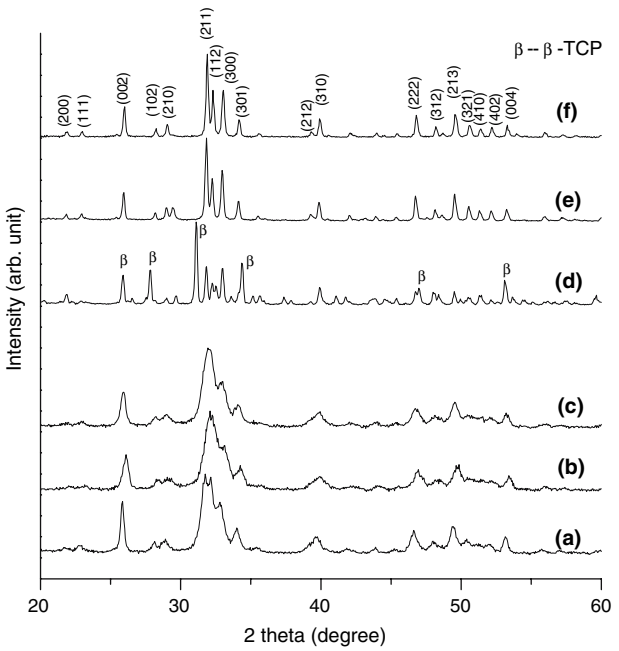

Fig. 3 XRD pattern of as received CHA (**a**), oven dried SHA (**b**), oven dried OHA (**c**) and 900 °C heated CHA (**d**), SHA (**e**) and OHA (**f**) powdered samples

nanocrystalline nature of microwave synthesized HAs. The crystallite sizes as listed in Table 1, also confirm the nanocrystalline nature of OHA. The fraction of crystalline phase (X_c) of HA was evaluated using the following formula [25], $X_c = 1 - (V_{112/300}/I_{300})$, where I_{300} is the intensity of (300) diffraction peak and $V_{112/300}$ is the intensity of the hollow between (112) and (300) diffraction peaks of HA. The X_c of OHA, SHA and CHA are listed in Table 1. The calculation shows that the crystalline fraction of OHA is slightly higher than SHA and CHA samples. This may be due to the biological origin of calcium carbonate used. The heat treated OHA and SHA has X_c of 0.91 and 0.9 respectively.

The FT-IR spectra of oven dried OHA, SHA and as received CHA samples are shown in Fig. 4. All the samples exhibits characteristic stretching and librational modes of OH^- groups at 3,571 cm^{-1} (ν_S) and 631 cm^{-1} (ν_L), whereas the internal modes corresponding to the PO_4^{3-} groups occur at: 1,088 and 1,046 cm^{-1} (ν_3), 962 cm^{-1} (ν_1), 599 and 560 cm^{-1} (ν_4) and 469 cm^{-1} (ν_2) corresponding to that of HA. The bands at 3,435 and 1,637 cm^{-1} correspond to adsorbed H_2O while bands at 1,482 and 1,424 cm^{-1} are that of CO_3^{2-} ions which suggests incorporation of carbonate ion in synthesized HA [26]. The cell parameter of OHA shows decreased *a*-axis characteristic of B-type carbonate ion substitution [27].

The SEM micrographs of OHA, SHA and CHA powder are shown in Fig. 5. From the SEM pictures, it is clearly observed that the precipitated crystallites of both the OHA and SHA were of spherulite morphology with narrow size distribution of about few micron in diameter, whereas CHA has flake like morphology of relatively larger size. The spherulite is composed of tiny nanosize platelets of loosely aggregated stabilized structure [18]. Hence, to characterize the morphology of the platelets, TEM analysis was done on ultrasonically dispersed OHA in ethanol. The bright field TEM image of oven dried OHA powder is shown in Fig. 6. The morphology clearly indicates that the particles are platelets, mostly agglomerated and of dimensions: length 33–50 nm and width 8–14 nm. This result thus clearly confirms the nanosize nature of OHA.

The specific surface area of the OHA, SHA and CHA obtained from the BET method is listed in Table 1. It is observed that both the microwave processed HA's had larger specific surface area than the commercially pure HA and can be attributed to their particle size and shape (Fig. 5). As the nano particle size decreases, the surface area increases which may be due to increased number of atoms occupying the surface. The specific surface area of OHA (106 m^2/g) has been found to be greater than reported value of around 34–80 m^2/g for nanocrystalline HA [28, 29]. The particle size was also calculated from BET specific surface area using the empirical equation $t = 6/(\rho \cdot S)$ (where t is the average grain size in micron, ρ the density in g/cm^3 and S the specific surface area in m^2/g) [28]. The values as listed in Table 1, again corroborates XRD and TEM results characterizing nano dimension of microwave synthesized HAs. The SEM picture of CHA shows the presence of flakes of micron size but calculations based on the XRD results and surface area measurements (Table 1) indicate nano size particles.

The in vitro dissolution study as shown in Fig. 7 indicates that all three HAs are stable in phosphate buffer solution at pH 7.2, except for the initial fluctuations. The

Table 1 List of cell parameter, crystallite size, fraction of crystalline phase (X_c), specific surface area, density and particle size of HAs

Sample	*a*(Å)	*c*(Å)	Crystallite size (nm)	Fraction of crystalline phase (X_c)	Surface area (m^2/g)	Density (g/cm^3)	Particle size (nm) based on BET
OHA	9.412	6.877	21	0.13	106	3.12	18
SHA	9.410	6.872	19	0.09	104	3.06	19
CHA	9.439	6.88	29	0.11	76	3.04	26

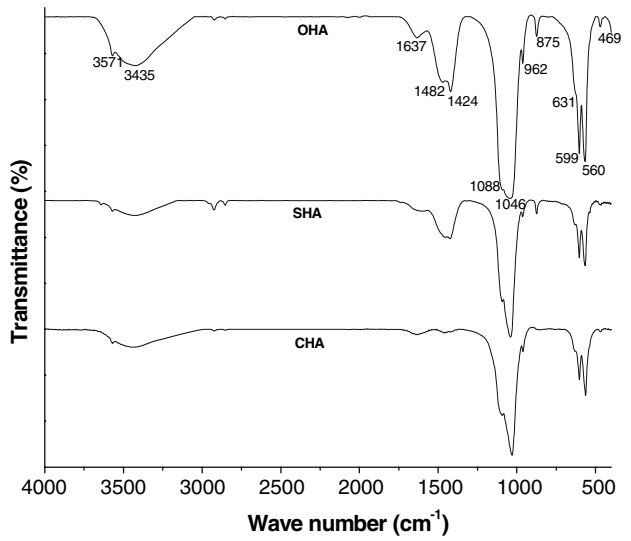

Fig. 4 FT-IR spectra of HA samples

that the Ca/P ratio of SHA may be less than the stoichiometric value and much lesser in case of CHA [29]. The initial increase in pH may be due to the surface dissolution of HA which releases OH^- ions into the solution [30]. Figure 8 shows the XRD patterns of the OHA, SHA and CHA samples after the in vitro solubility study. As there is no change in the patterns before and after the in vitro study, this also confirms that all the three HAs are stable in body fluids. Though the XRD and FTIR show similarity among the three HAs, the SEM, surface area measurement, and in vitro studies clearly indicate the microwave processed OHA has better properties than SHA and CHA.

The sinterability of OHA has been studied from 800 to 1,250 °C and the results are compared with SHA and CHA samples. The XRD patterns of the OHA pellets sintered at different temperatures are shown in Fig. 9. The peak positions in all the patterns from 800 to 1,200 °C

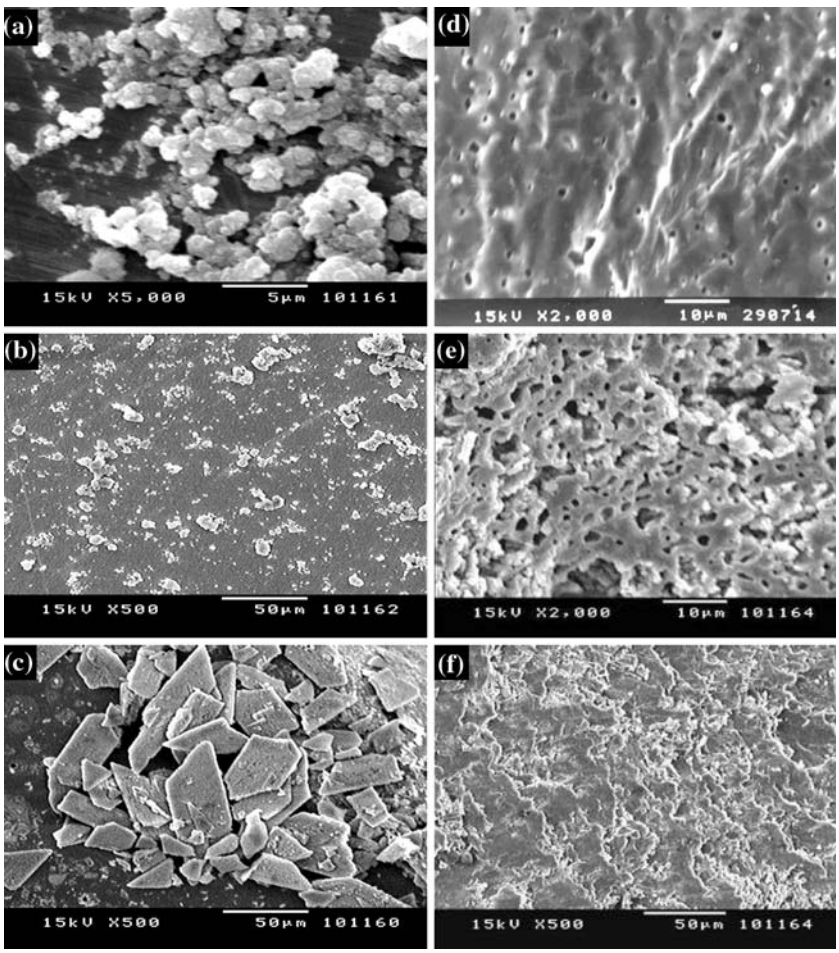

Fig. 5 SEM micrographs of (**a**) OHA (**b**) SHA (**c**) CHA powder and fractured surfaces of OHA (**d**), SHA (**e**) and CHA (**f**) pellets sintered at 1,200 °C

CHA solubility curve lies below that of SHA and the SHA curve itself lies below that of OHA. As the stoichiometric HA is very stable at pH 7.2, the present results, indicates

correspond to the pure HA, where as the XRD pattern of the pellet sintered at 1,250 °C shows a decrease in the intensity of the HA and the presence of additional peaks at

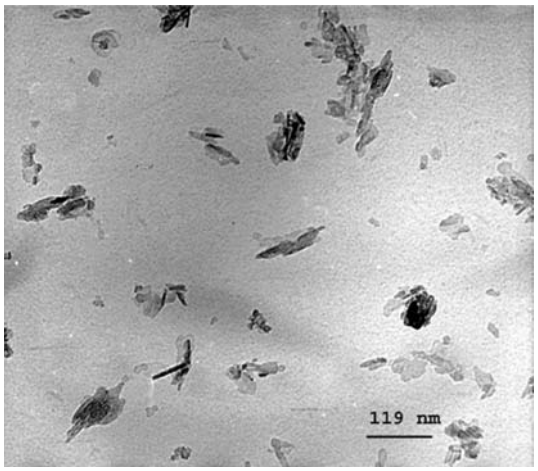

Fig. 6 TEM bright field image of OHA powder sample

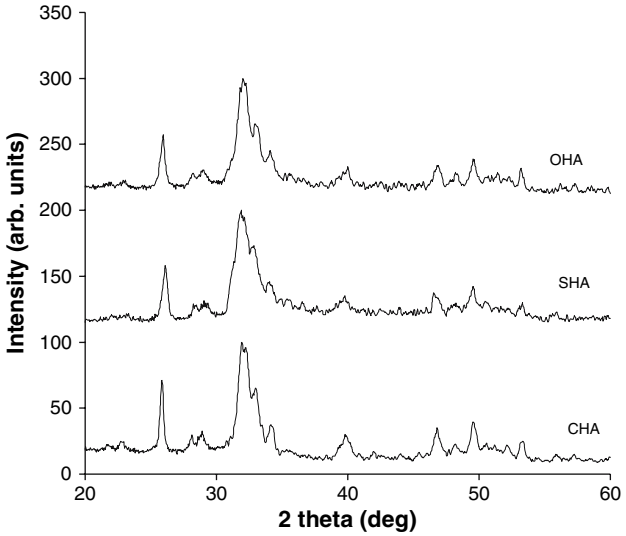

Fig. 8 XRD pattern of HA samples after dissolution

37.3 and 55.3°, corresponding to the major peaks of calcium oxide (CaO) i.e. (2 0 0) and (2 2 0) (JCPDS 37-1497). So from the figure it appears that the OHA seems to decompose at around 1,250 °C. The XRD patterns of the sintered pellets of SHA as a function of sintering temperature are shown in Fig. 10. Similar to OHA, SHA is also stable upto 1,200 °C but the 1,250 °C pattern shows the presence β-TCP as the major phase. Figure 11 shows the XRD patterns of sintered CHA pellets at the above-mentioned temperatures. The β-TCP appears as a major phase at 900 °C. The allotropic transformation of β-TCP to α-TCP (9-348 JCPDS) was observed for CHA samples sintered at 1,250 °C with the appearance of peaks of α-TCP along with β-TCP. The formation of TCP during sintering of SHA and CHA indicates that their Ca/P molar ratio is below 1.67. Similarly the presence of CaO during the sintering of OHA indicates that the Ca/P ratio could be slightly exceeding 1.67. Although both OHA and SHA were prepared under similar procedure, they exhibit different stoichiometric values as evident from dissolution and sintering studies. The near stoichiometric Ca/P ratio observed in OHA may be due to the nature of the calcium precursor. The presence of β-TCP in the CHA even at 900 °C clearly indicates that the Ca/P ratio is much lower than the stoichiometric value [24].

The variation of density of HA pellets as a function of sintering temperature is shown in Fig. 12. The OHA has a maximum density at 1,200–1,250 °C, which has been found to be comparable with the reported value for sintered pellets of nanocrystalline HA (98% of the theoretical density) [28]. At this temperature, OHA has 98.8% of the theoretical density of HA (3.156 g/cm^3, JCPDS 9-432), whereas SHA has 97% of its theoretical density. The density of CHA continuously increases with sintering temperature and corresponds to the density of β-TCP phase (3.07 g/cm^3, JCPDS 9-169). The reason for the good compactness of OHA and also SHA is due to their particle morphology i.e., both HAs have spherulite structure.

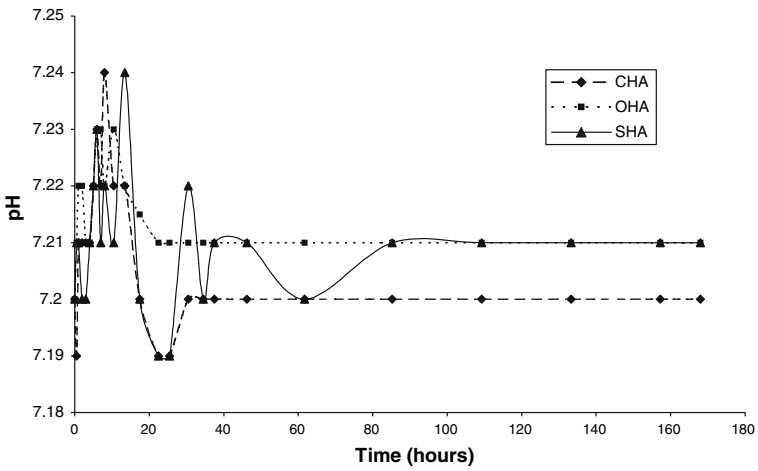

Fig. 7 Variation in pH of phosphate buffer due to the immersion of HA samples

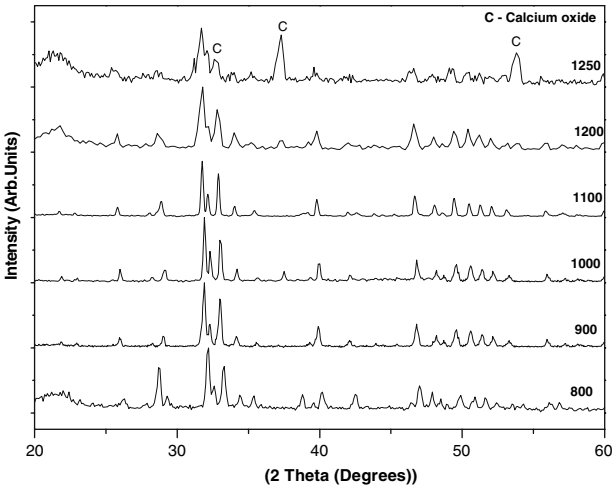

Fig. 9 XRD patterns of the sintered pellets of OHA

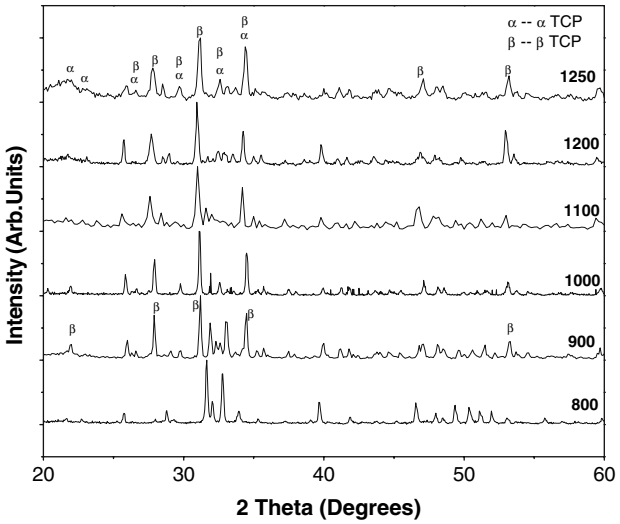

Fig. 11 XRD patterns of the sintered pellets of CHA

The density of SHA is less than that of OHA at all sintering temperatures may be due to porosities associated with it. The density of CHA is less than that of SHA as well as OHA and may arise due to decomposition to HA and β-TCP where density of latter is less. At sintering temperature of 1250 °C the OHA density does not vary even with presence of CaO (3.35 g/cm^3, JCPDS 37-1497), but the SHA shows a dip in density due to β-TCP formation. The apparent increase in the density of CHA with sintering temperature even at 1,250 °C is not because of HA but due to good sinterability of β-TCP and also due to the allotropic transformation of β-TCP to α-TCP (2.87 g/cm^3, JCPDS 9-348) [24].

The variation in hardness values of the pellets of the three HAs with sintering temperature is shown in Fig. 13. The OHA has a maximum hardness value of 445 Hv at 1,200 °C. The CHA has a maximum hardness value of 352 Hv at 1,100 °C and gradually decrease to 338 Hv at 1,200 °C. Although SHA seems to have the lowest hardness above 1,000 °C compared to that of OHA and CHA, it should be noted that CHA has already decomposed and the hardness corresponds to that of β-TCP. The observed decrease in hardness of the OHA at 1,250 °C is due to CaO formation while the decrease above 1,100 °C in case of CHA may be due to phase transformation of β-TCP to α-TCP [24]. The lower hardness value of SHA may be due to porosities. The high hardness of the OHA indicates its good sinterability.

The SEM photographs of the freshly fractured surface of the OHA, SHA and CHA pellets sintered at 1,200 °C are shown in Fig. 5d–f. The fractured surface of OHA shows

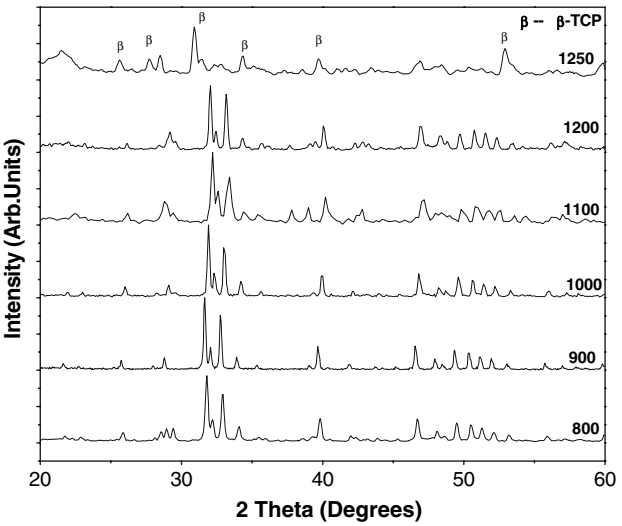

Fig. 10 XRD patterns of the sintered pellets of SHA

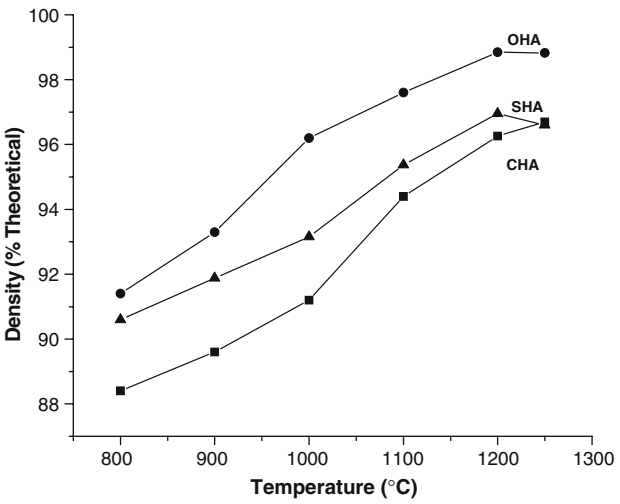

Fig. 12 Density variation of HA pellets with sintering temperatures

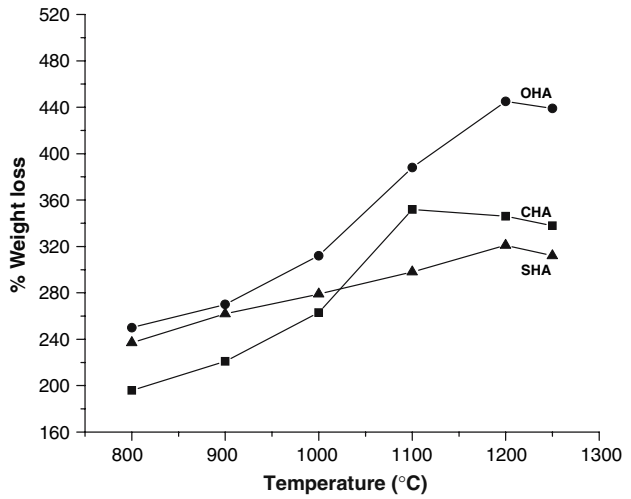

Fig. 13 Hardness variation of HA pellets with sintering temperatures

depressions due to intergranular fracture. The OHA agglomerates of spherulites as observed in Fig. 5a increases the compactness of the material, which in turn favours the high density of the pellet. The fracture surface of SHA exhibits presence of more pores, which are responsible for the lowering its density and hardness values. The characteristic fracture surface of the CHA clearly indicates that it is an intragranular fracture. Although the XRD analysis of the sintered pellets show that both the microwave processed HAs are stable at high temperatures, the hardness and density values clearly indicates that OHA has superior sintering properties than the SHA and CHA.

The results of the qualitative evaluation of the in vitro cytotoxicity test of the apatite samples are listed in Table 2. The osteoblast cell culture study was carried out on HA pellets sintered at 900 °C. Since OHA and SHA were stable at 900 °C, cell culture was evaluated on these samples. The MG-63 osteoblast cells around the OHA and SHA samples showed normal response as cells around negative control material (Table 2). The presence of more osteoblast cells was observed on the surface of the OHA compared to SHA after the incubation period of a day as shown in the micrographs (Fig. 14). Thus OHA has been found to be noncytotoxic and favouring adhesion of osteoblast cells. Overall, the OHA seems to have better properties compared to SHA. The biological origin of

Table 2 Qualitative evaluation of in vitro cytotoxicity test

Sample	Cytotoxicity scale	Interpretation
Negative control	0	Noncytotoxic
Positive control	3	Severely cytotoxic
OHA	0	Noncytotoxic
SHA	0	Noncytotoxic

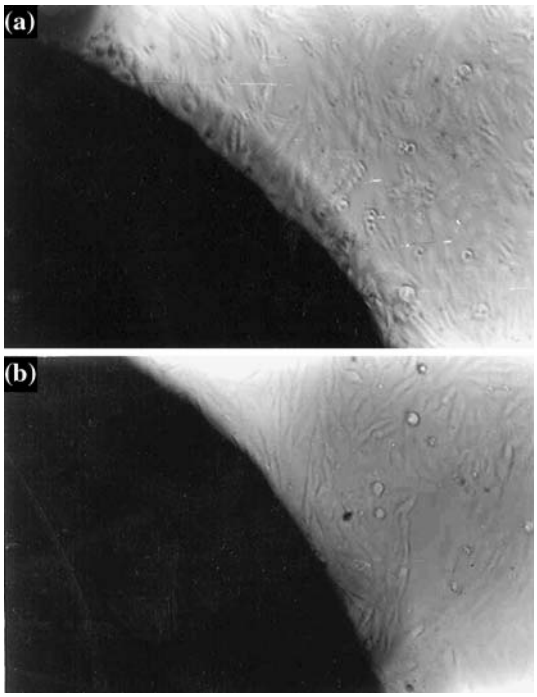

Fig. 14 Photographs of OHA (**a**) and SHA (**b**) pellets with osteoblast cells

calcium carbonate, arising from the use of eggshell in synthesis, may play a role in improving the properties of OHA.

Conclusions

Nanocrystalline hydroxyapatite (OHA) has been successfully synthesized from eggshell waste using microwave irradiation. Compared to the SHA and CHA, the OHA seems to have better morphology, stoichiometry, sinterability, stability at high temperatures and osteoblast cell adhesion. The eggshell seems to be a promising source of calcium for preparing nanocrystalline hydroxyapatite with excellent properties so essential for hard tissue replacement.

References

1. B. BEN-NISSAN, *Curr. Opinion Solid State Mater. Sci.* **7** (2003) 283
2. L. DUPOIRIEUX, *Br. J. Oral Maxillofac. Surg.* **37** (1999) 467
3. L. SEVGI OZYEGINA, F. N. OKTARB, G. GOLLERC, E. SABRI KAYALIC and T. YAZICI, *Mater. Lett.* **58** (2004) 2605
4. S. JOSCHEK, B. NIES, R. KROTZ and A. GÖPFERICH, *Biomaterials* **21** (2000) 1645
5. F.-H. LIN, C.-J. LIAO, K.-S. CHEN and J.-S. SUN, *Biomaterials* **20** (1999) 475
6. M. OZAWA and S. SUZUKI, *J. Am. Ceram. Soc.* **85** (2002) 1315

7. D. M. ROY and S. K. LINNEHAN, *Nature* **247** (1974) 220
8. M. SIVAKUMAR, T. S. SAMPATH KUMAR, K. L. SHANTHA and K. PANDURANGA RAO, *Biomaterials* **17** (1996) 1709
9. E. M. RIVERA, M. ARAIZA, W. BROSTOW, V. M. CASTANO, J. R. DIAZ-ESTRADA, R. HERNANDEZ and J. ROGELIO RODRIGUEZ, *Mater. Lett.* **41** (1999) 128
10. G. GOLLER, F. N. OKTAR, L. S. OZYEGIN, E. S. KAYALI and E. DEMIRKESEN, *Mater. Lett.* **58** (2004) 2599
11. S. J. LEE and S. H. OH, *Mater. Lett.* **57** (2003) 4570
12. Y. HAN, K. XU, G. MONTAY, T. FU and J. LU, *J. Biomed. Mater. Res.* **60** (2002) 511
13. T. J. WEBSTER, C. ERGUN, R. H. DOREMUS, R. W. SIEGEL and R. BIZIOS, *Biomaterials* **22** (2001) 1327
14. J.C. JANSEN, A. ARAFAT, A. K. BARAKAT and H. VAN BEKKUM, in *Synthesis of Microporous Materials*, vol. 1, M. L. Occelli and H. Robson (eds) Van Nostrand Reinhold, New York, 1992, p. 507.
15. K. J. RAO, B. VAIDHYANATHAN, M. GANGULI and P. A. RAMAKRISHNAN, *Chem. Mater.* **11** (1999) 882
16. T. S. SAMPATH KUMAR, I. MANJUBALA and J. GUNASEKARAN, *Biomaterials* **21** (2000) 1623
17. A. L. MACIPE, J. G. MORALES and R. R. CLEMENTE, *Adv. Mater.* **10** (1999) 49
18. S. SARIG and F. KAHANA, *J. Cryst. Growth* **55** (2002) 237
19. Z. YANG, Y. JIANG, Y. J. WANG, L. MA and F. LI, *Mater. Lett.* **58** (2004) 3586
20. J. LIU, K. LI, H. WANG, M. ZHU and H. YAN, *Chem. Phys. Lett.* **396** (2004) 429
21. A. SIDDHARTHAN, S. K. SESHADRI and T. S. SAMPATH KUMAR, *J. Mater. Sci. Mater. Med.* **15** (2004) 1279
22. J. PENA, R. Z. LEGEROS, R. ROHANIZADEH and J. P. LEGEROS, in Bioceramics, vol. 13. S. Giannini and A. Moroni (eds) Trans Tech Publications, Switzerland, 2001, pp. 267–70.
23. Y. FANG, D. K. AGRAWAL and D. M. ROY, in Hydroxyapatite and Related Materials, P. W. Brown and B. Constantz (eds) CRC Press, London, 1994, p. 269
24. S. RAYNAUD, E. CHAMPION, J. P. LAFON and D. BERNACHE-ASSOLLANT, *Biomaterials* **23**(2002) 1081
25. E. LANDI, A. TAMPIERI, G. CELOTTI and S. SPRIO, *J. Eur. Ceram. Soc.* **20** (2000) 2377
26. S. KOUTSOPOULOS, *J. Biomed. Mater. Res.* **62** (2002) 600
27. R. ZAPANTA-LEGEROS, *Nature* **206** (1965) 403
28. L. B. KONG, J. MA and F. BOEY, *J. Mater. Sci.* **37** (2002) 1131
29. E. MAVROPOULOS, A. M. ROSSI, N. C. C. DA ROCHA, G. A. SOARES, J. C. MOREIRA and G. T. MOURE, *Mater. Character.* **50** (2003) 203
30. J. H. CHERN LIN, K. H. KUO, S. J. DING and C. P. JU, *J. Mater. Sci. Mater. Med.* **12** (2001) 731